

Structural distortion in superconducting $\text{Ba}_{1-x}\text{K}_x\text{BiO}_3$

M. Braden,^{1,2} W. Reichardt,¹ E. Elkaim,³ J. P. Lauriat,³ S. Shiryayev,⁴ and S. N. Barilo⁴

¹Forschungszentrum Karlsruhe, IFP, Postfach 3640, D-76021 Karlsruhe, Germany

²Laboratoire Léon Brillouin, C.E.A./C.N.R.S., F-91191 Gif-sur-Yvette CEDEX, France

³LURE, Université Paris-Sud, 91405 Orsay Cedex, France

⁴Institute of Physics of Solids and Semiconductors, Acad. Sci., P. Brovki 17, Minsk 220072, Belarus

(Received 14 March 2000)

The structure of superconducting $\text{Ba}_{1-x}\text{K}_x\text{BiO}_3$ (BKBO) has been studied by neutron and synchrotron diffraction on single crystalline and on powder samples. In contrast to the phase diagram reported by several groups we find a long range structural distortion persisting in the K-concentration range of superconductivity. The distortion is characterized by a tilt of the BiO_6 octahedra around the cubic [001] direction, space group $I4/mcm$, so far not observed for any BKBO compound. The mixing of light monovalent K atoms with the heavier two-valent Ba atoms causes strong structural disorder, in particular for the octahedron tilt. This disorder is simulated within a harmonic lattice dynamical model.

I. INTRODUCTION

K-doped BaBiO_3 is a prominent material in the context of high temperature superconductivity since it exhibits a high transition temperature^{1,2} and since in contrast to the cuprates one has to exclude a magnetic mechanism. Though there are several arguments in favor of an electron lattice mechanism like a sizeable isotope effect³ and strong phonon renormalization induced by the doping,^{4,5} the combination of high T_c and low electronic density of states points to an unconventional pairing.⁶

The phase diagram of BKBO has been studied by several groups mainly by powder neutron diffraction.^{7,8} It is stated that superconductivity exists only in the structurally undistorted cubic phase for K concentrations higher than 0.3. For lower concentrations one observes a structural distortion characterized by the tilt of the octahedra around a cubic [110] axis, space group $Ibmm$. Electronically, the $Ibmm$ phase is not only characterized by the disappearance of superconductivity but also by a nonmetallic behavior which, however, may not be attributed to the tilt distortion. It is frequently argued that the charge disproportionation responsible for the insulating behavior in the pure compound⁹ persists on a short range scale in the $Ibmm$ phase. Since the charge disproportionation is related to the structural breathing distortion, an alternation of large and small BiO_6 octahedra, this distortion should also be found in the $Ibmm$ phase as it was claimed on the ground of EXAFS experiments.^{10,11} Further strong support for this view arises from Raman scattering:^{12,13} in undoped BaBiO_3 there is a dominant peak in the spectra which should be interpreted by the breathing mode becoming Raman-active due to the distortion (note that a cubic perovskite has no Raman-active mode). The frequency of this peak agrees nicely with the observation by neutron scattering.¹⁴ The Raman-spectra in the intermediate $Ibmm$ -phase still show this peak though the long range breathing distortion disappears at smaller K concentration. In the superconducting phase which is reported to be structurally undistorted, i.e., cubic, only weak indications for local breathing distortions can be found in Raman scattering.

In this paper, we report the results of several diffraction

studies in the superconducting concentration range which demonstrate that there still is a structural distortion. The structural difference between superconducting and non-superconducting BKBO appears to consist in the direction of the tilt axis, though the structural details of the phase boundary still need clarification. The competition between different tilt schemes and superconductivity resembles closely the observation in the Pb-doped BaBiO_3 compounds (BPBO) (Ref. 15) and it may also be related to the suppressed superconductivity in some LTT-phase cuprates.¹⁶

II. EXPERIMENT

Single crystals of BKBO were obtained by electrochemical decomposition described in Refs. 17,18. The basic characteristics of the used samples are summarized in Table I. In order to perform neutron diffraction and scattering studies within reasonable counting time crystals with large sample volumes were grown in Minsk for different K concentrations. A smaller sample was grown at Clarendon Laboratory, Oxford, in the aim of optimizing the superconducting properties. T_c and the superconducting transition widths of

TABLE I. Characteristic properties of the different used $\text{Ba}_{1-x}\text{K}_x\text{BiO}_3$ crystals. Superconducting transition temperatures were determined by SQUID or by ac susceptibility measurements. Int. ratio denotes the ratio of the intensities of the (1.5 0.5 0.5) and the (2 0 0) reflections.

x -K	label	weight	a (Å)	T_c (K)	ΔT_c (K)	T_s (K)	Int. ratio
0.324(5)	A	6.4g	4.2984	^a	/	245(10)	1.5%
0.355(5)	B	0.16g	4.2930	32.5	5.8	200(10)	1.0%
0.363(5)	C	1.7g	4.2916	28.5	4.1	182(10)	0.5%
0.369(5)	D	0.5g	4.2904	27	10	220(10)	1.3%
0.403(5)	E	4.6g	4.2845	29.5	5.9	140(13)	0.4%
0.410(5)	F	2.6g	4.2834	23.1	4.8	145(15)	0.3%

^aIn ac susceptibility only a signal an order of magnitude smaller than that in the other crystals was found in the temperature range 6–28 K.

the crystals B, C, E, and F are comparable to the best values reported for powder samples. The most reliable determination of the K content can be performed by measuring the pseudocubic lattice constant a_p , and by analyzing it with the relation

$$a_p = 4.3548 - 0.1743x, \quad (1)$$

obtained by Pei *et al.*⁸ on powder samples.

Neutron scattering studies were performed at the ORPHEE reactor using the triple spectrometers 2T (thermal source), G4.3, 4F2 (cold source), and the two axis diffractometer 3T1 (thermal source). In all experiments pyrolytic graphite monochromators were used (in the case of 2T double focusing, in the case of 4F2 a double monochromator) and in the triple axis experiments focusing or double focusing graphite analyzers. In order to suppress the higher order contaminations with a pyrolytic graphite filter, the final energy was fixed to 14.7 meV. Samples were oriented with the [100] and the [011] directions parallel to the diffraction plane.

In addition a large set of Bragg-reflection intensities was collected on the four-circle diffractometer 5C2 allowing a complete structure analysis at 50, 295, and 450 K. This diffractometer is installed at a hot source and uses a Cu(220) monochromator ($\lambda = 0.808 \text{ \AA}$), which permits to extend the data collection to rather high Q values. Powder diffraction studies using synchrotron radiation were performed at the Wiggler beam-line DW22 at the LURE using samples obtained by grinding parts of the above described crystals.

III. RESULTS AND DISCUSSION

Temperature dependence of superstructure reflection intensities. The first indication of a structural distortion in superconducting samples of BKBO was found during a four circle experiment on the small crystal with low mosaic spread (crystal D, see Table I). With the four circle diffractometer it has been possible to follow distinct superstructure reflections, (1.5 1.5 2.5) and (2.5 1.5 1.5) in cubic notation, as a function of temperature. The results are shown in Fig. 1. Without any knowledge of the low symmetry space group one may argue that these distinct reflections arise from different domains in the low-temperature phase. Differences in the intensities below $T_s = 220 \text{ K}$ are explained by unequal domain volumes. The character of this transition has to be identified with an octahedron rotation similar to the one observed by powder neutron diffraction for smaller K content. Close inspection of Fig. 1 shows that there is still significant intensity at higher temperature which renders the determination of the critical temperature difficult. In the lower part of Fig. 1 we show the temperature dependence of the Q - and energy-width of scans through this superstructure intensity performed on the triple axis spectrometer 4F2. The widths below $\sim 200 \text{ K}$ correspond to the experimental resolution, however, the scattering becomes broadened in Q space and in energy when the temperature is close to or increased above T_s . In principle, this corresponds to the usual critical scattering around a second order phase transition, and it nicely agrees with the observation on the four-circle diffractometer: above the transition the domain structure is lost and the observed intensities reflect the cubic symmetry.

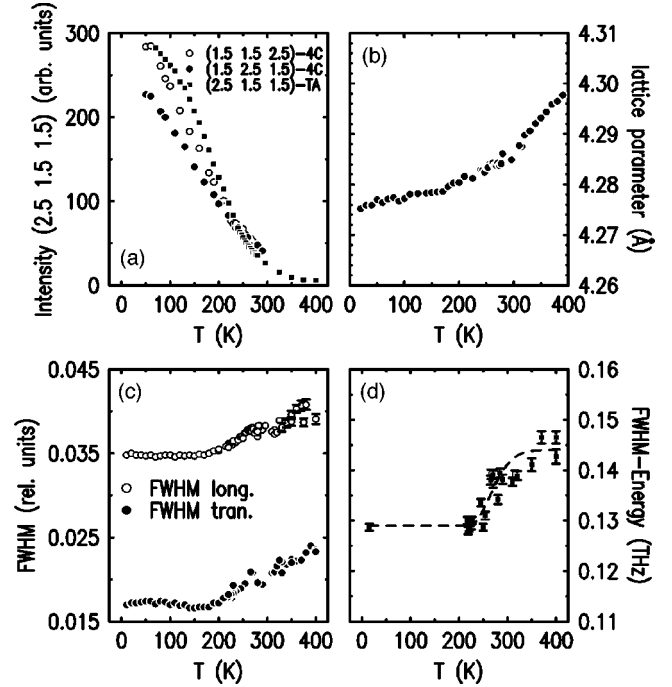


FIG. 1. Results obtained with the small crystal D of composition $\text{Ba}_{0.63}\text{K}_{0.37}\text{BiO}_3$: (a) Temperature dependence of the superstructure reflection intensities measured on the four-circle, denoted by open and filled circles (4C), and on the triple axis spectrometer, denoted by squares (TA). (b) pseudocubic lattice constant as function of temperature; (c) full width at half maximum (FWHM) of scans performed across the superstructure reflections in longitudinal and transverse direction; (d) FWHM of energy scans performed across the superstructure reflections.

What appears rather anomalous in the structural transition in BKBO is the extension of the critical region; the critical scattering can be followed up to 400 K, i.e., close to twice T_s . Constant energy scans with higher statistics in a second run of experiments on 4F.2 have been fitted by a Lorentzian $[(Q - Q_0)^2 + \kappa^2]^{-1}$, convoluted with the experimental resolution. The temperature dependence of κ and the corresponding correlation length of the fluctuations ξ are shown in Fig. 2. Even at temperatures almost 200° higher than the thermodynamic transition the fluctuations are characterized by a rather large length scale. Below we will show that the symmetry of the low-temperature phase corresponds to space group $I4/mcm$. Concerning the symmetry the transition is hence identical to the one observed in SrTiO_3 ,¹⁹ however, in this compound the critical scattering is restricted to the region $0.95T_s - 1.05T_s$. The reason for the pronounced smearing of the transition in BKBO can be found in the disorder induced by the Ba-K mixing which yields strong effects in the case of BKBO since the charges are varying by a factor of 2 and the masses by a factor of 3.5 (ionic radii are almost identical²⁰). Similar effects are observed for $(\text{La}/\text{Sr})_2\text{CuO}_4$, although the Sr content there is much smaller than the K content in BKBO and the differences in charge are smaller. The smearing of the transition or the pinning of fluctuations in BKBO may be compared to ferroelectric relaxor materials,²¹ where the ferroelectric transition is essentially influenced by substitution disorder. Our simulations of the structural disorder due to Ba-K mixing confirm a strong in-

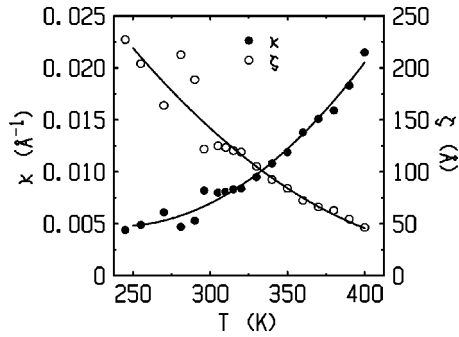


FIG. 2. Half width at half maximum κ of the Lorentzian profiles fitted to the measured scans across the (2.5 1.5 1.5)-superstructure reflection in $\text{Ba}_{0.63}\text{K}_{0.37}\text{BiO}_3$ (left scale, filled circles). The scans were performed in longitudinal direction, and in order to describe the measured peak shape the Lorentzian profile was convoluted with the experimental resolution. The measurements were performed on the triple axis spectrometer 4F.2. With the right scale we present the temperature dependence of the corresponding correlation length.

fluence on the octahedron tilt and the corresponding transition, see below.

The pseudocubic lattice constant recorded in the 4F2 experiment shows no sizeable anomaly related to the structural phase transition, see Fig. 1. The same type of superstructure is observed in the whole series of examined crystals. The left part of Fig. 3 shows the results of measurements on the triple axis spectrometer G43 using large crystals of different composition (crystals A, C, and F, see Table I) all of them show the structural distortion with a similar smearing as the one discussed above. For one of the crystals $Fx=0.41$, the measurements upon cooling and upon heating did not reveal any hysteresis. In contrast, the experiment on the smaller crystal D revealed different intensities for successive cooling cycles which we attribute to nonreproducible domain ratios. In the larger crystal these effects should be averaged. For these large crystals A, C, E, and F, one may hence assume almost

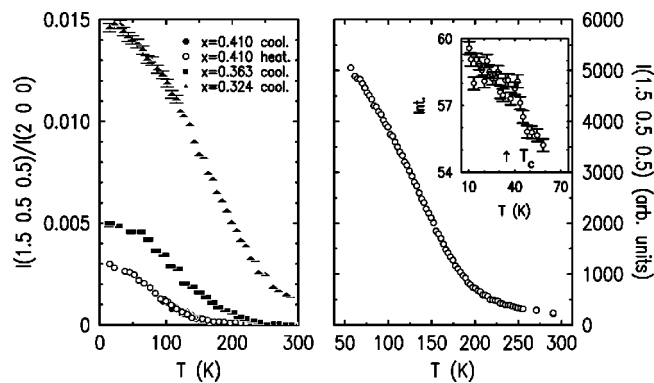


FIG. 3. Left part: temperature dependence of the superstructure reflection intensities (1.5 0.5 0.5) scaled to the intensity of the (2 0 0)-Bragg reflection in three large crystals of BKBO with $x=0.41$, 0.363, and 0.324, crystals A, C, and F. For $x=0.41$ data has been collected upon heating and upon cooling. Right part: temperature dependence of the superstructure reflection intensity in the small crystal of composition $\text{Ba}_{0.645}\text{K}_{0.355}\text{BiO}_3$, B, which exhibits a sharp superconducting transition at $T_c=32.5$ K. The inset shows the intensity data close to the superconducting transition.

TABLE II. Results of the structural analyses on crystal D with composition $\text{Ba}_{0.63}\text{K}_{0.37}\text{BiO}_3$; in the cubic phase ($Pm\bar{3}m$, 450 and 295 K) the sites are Bi at (0,0,0), Ba at (0.5 0.5 0.5), and O at (0,0,0.5). In the $I4/mcm$ phase the lattice corresponds to $\sqrt{2}a \times \sqrt{2}a \times 2a$, there is one oxygen at (0.25+x, 0.25-x, 0) and another one at (0,0,0.25), the thermal parameters of these were constrained to be identical.

T (K)	450	295	50
$R_w/R_{unw}(\text{Int.})$	2.42%/1.70%	2.63%/1.74%	4.21%/3.63%
Indep. Reflections	78	87	789
Ba-U (\AA^2)	0.0142(3)	0.0099(1)	0.0040(1)
Bi-U (\AA^2)	0.0052(1)	0.0038(1)	0.00196(6)
O-U ₁₁ (\AA^2)	0.0302(3)	0.0237(2)	0.0123(1)
O-U ₃₃ (\AA^2)	0.0088(2)	0.0070(1)	0.0057(1)
O1-x			0.01511(9)

equal domain fractions and discuss the relative intensities of the superstructure reflections. The transition temperature may be defined as the crossing between a linear temperature dependency below T_S and and the linear extrapolation of the temperature dependence of the critical scattering above T_S . The so-determined transition temperature is slightly above the temperature where the broadening of the intensity distribution in Q space sets in. However, it may be seen in Fig. 3 that the transition becomes more sluggish with increasing K content which impairs the determination of a critical temperature. The transition temperature and the intensity normalized to that of the (200) fundamental reflection at low-temperature decrease with increasing K concentration in agreement to the observation at lower K content in powder neutron diffraction.⁸ The K doping unfavors the octahedron tilt. One may note that the superstructure intensities are very weak which might render their detection by powder neutron diffraction difficult.

The superstructure reflection was also found in the small sample B presenting a very sharp and high superconducting transition. This confirms once more that the distortion is co-existing with superconductivity. The right part of Fig. 3 shows the temperature dependence of that intensity with the inset presenting the data close to T_c , where, however, no anomaly could be detected within the statistical errors.

Determination of the low temperature space group. Two independent studies, single crystal neutron diffraction and powder diffraction using synchrotron radiation, were used to determine the space group to $I4/mcm$. With the smaller crystal D, which has a sufficiently low mosaic spread, we have performed structure analyses at 50, 295, and 450 K, measuring sets of 859, 812, and 926 Bragg reflection intensities, respectively. The data sets at 295 and 450 K, i.e., in the cubic phase could be treated by the standard techniques³⁰ and the results are given in Table II. Half spheres of reflections were measured up to 106° and 98° in 2Θ at 295 and at 450 K, respectively [corresponding to $(\sin(\Theta)/\lambda)_{\text{max}}=0.98$ and 0.93, respectively]. The data sets were averaged according to the Laue-group $m\bar{3}m$ yielding 87 and 78 independent reflections with very low internal R values of 1.24 and 1.26 %, respectively. The data was corrected for absorption and an extinction correction was refined according to the Becker-Coppens formalism of type I; all refinements were

performed with the PROMETHEUS program package.²² As already indicated by the exceptionally low internal R values, the corrections are relatively small. In addition, the anisotropic atomic displacement parameters, the Ba/K and the oxygen occupation was varied. The Ba/K occupations refined with the 450, 295, and the 50 K data indicate a K concentration of 0.38(3), 0.39(3), and 0.35(2), respectively (we have used $b_{\text{Ba}}=0.517$ fm and $b_{\text{K}}=0.371$ fm) with its largest error arising from the uncertainty of the Ba scattering length. For the O occupation we find 0.995(5) and 1.004(5) at 295 and at 450 K, respectively,²³ confirming that the electrochemically synthesized crystals have an almost stoichiometric O content, which is expected due to the high effective O-partial pressure at the growth electrode.

In the case of the 50 K experiments the data were collected in the $2a_p \times 2a_p \times 2a_p$ lattice with a_p the perovskite cubic lattice constant, an eighth of a sphere was measured up to $2\Theta = 78^\circ$, at higher angles only reflections corresponding to a F-centered lattice were measured. The intensity data may be described within the cubic perovskite, however, the large number of observed superstructure reflections results in a high R value of 13.7%. A major complication for the 50 K data analysis within distorted models arises from the twinning which superposes the contributions of different domains similar to the situation in $(\text{La}/\text{Sr})_2\text{CuO}_4$.²⁴ There is no splitting of the Bragg reflections detected within the resolution of the four-circle diffractometer 5C2. Therefore, it is ascertained that the measured intensities correspond to the integration over all domains. The data were averaged according to Laue group mmm in order to maintain the information of the domains for a tetragonal as well as for an orthorhombic low temperature structure yielding 789 independent reflections and a low internal R value of 1.61%. In analogy to the phase diagram for BPBO (Ref. 15) and the low K-content part of that of BKBO (Ref. 8) one may consider two possible space groups: $I4/mcm$ and $Ibmm$. In both lattices the two shorter parameters arise from the cubic perovskite by $\sqrt{2} \times a_p$ and the longer by $2a_p$. In the case of the tetragonal space group $I4/mcm$ associated with a tilt of the octahedra around $[001]$, one has to consider three different orientations though the real twinning law is more complex. These three arrangements correspond to the orientation of the tetragonal axis along $[100]$, $[010]$, or $[001]$ of the cubic perovskite. The calculation may be easily performed using the nonstandard F -centered setting (corresponding to $2a \times 2a \times 2a$); a measured intensity has then to be fitted by

$$\text{Int}(h \ k \ l) = \text{scale}[\alpha F^2(h \ k \ l) + \beta F^2(h \ l \ k) + (1 - \alpha - \beta)F^2(l \ k \ h)], \quad (2)$$

where α, β designate the volume fractions of the different domains and $F(hkl)$ is the structure factor of the (hkl) reflection.

The results of the refinements with the 789 reflections are given in Table II in the standard setting $I4/mcm$. The description of the data within space group $Ibmm$ is more difficult since the twinning is more complex. For the analysis of the twinning, one may consider that each of the tetragonal twin domains splits into two domains as in a tetragonal to orthorhombic transition leading to six orientations. (This should not be confused with the total symmetry reduction

where $I4/mcm$ and $Ibmm$ are at the same level.²⁶) The measured intensities have then to be fitted by a sixfold superposition

$$\begin{aligned} \text{Int}(hkl) \propto & \alpha F^2(h, k, l) + \beta F^2(k, h, l) + \gamma F^2[0.5(h+k \\ & + l), 0.5(h+k-l), (h-k)] + \delta F^2[0.5(h+k \\ & - l), 0.5(h+k+l), (h-k)] + \epsilon F^2[0.5(h-k \\ & + l), 0.5(h-k-l), (h+k)] \\ & + (1 - \alpha - \beta - \gamma - \delta - \epsilon) \cdot \\ & F^2[0.5(h-k-l), 0.5(h-k+l), (h+k)]. \quad (3) \end{aligned}$$

The data can be described reasonably well within the $Ibmm$ model, however, the R values are significantly higher in spite of the greater number of free parameters in the orthorhombic model $R_w(\text{Int.})=4.50\%$ and $R_{uw}(\text{Int.})=3.81\%$ compared to $R_w(\text{Int.})=4.21\%$ and $R_{uw}(\text{Int.})=3.63\%$ in the tetragonal model. The R value test which is more significant than those found in the powder diffraction data at lower K concentration,⁸ suggests that the low-temperature space group is $I4/mcm$. In the case of the Rietveld-powder refinement the orthorhombic space group is favorable for refining the profiles and will impair the symmetry analysis.⁸ Within the $I4/mcm$ model one obtains a single tilt angle of 3.46° and in $Ibmm$ one determines two angles at the two distinct O positions 3.15° and 3.61° . $I4/mcm$ corresponds to a tilt around a $[001]$ axis or around a Bi-O bond whereas $Ibmm$ corresponds to a tilt around the $[110]$ axis or around a line parallel to the octahedron edge. Due to the superposition induced by the twinning the difference in the quality of the description is not essential though still significant.

The thermal parameters at all temperatures are rather large and will be discussed below. However, our results at 50 K may be compared to those of Kwei *et al.*²⁵ obtained on a powder sample of similar composition. Kwei *et al.* analyze their data in the cubic undistorted symmetry and obtain a very large value for the thermal parameter of the O site in the direction of the displacement by the tilt $U_{11}(\text{O})=U_{22}(\text{O})=0.0191(2) \text{ \AA}^2$ corresponding to a root mean square displacement of 0.14 \AA or a root mean square tilt of 3.5° . The large magnitude of the thermal parameter and the simple crystal structure allow a reliable determination with powder diffraction. Our refinements of the undistorted model with the single crystal data yield a comparably large value $0.0179(3) \text{ \AA}^2$. It is obvious that in our cubic treatment the enhanced parameter arises from the neglect of the distortion. The fact that Kwei *et al.*²⁵ find the same value clearly indicates that their sample exhibits a similar structural distortion.

In order to confirm the tetragonal space group we have performed synchrotron diffraction studies on powders obtained by grinding small parts of the crystals cut from opposite corners. The observed peak shapes remained in all cases larger than the experimental resolution of about 0.06 degrees full width at half maximum (FWHM) in 2Θ . The samples were inserted in a closed cycle refrigerator for cooling, and in order to reduce the influence of single grain scattering the sample was kept continuously oscillating. Complete patterns were recorded with a wavelength of 1.066 \AA ($10 < 2\Theta < 100^\circ$) at only a few temperatures for a part of crystal A.

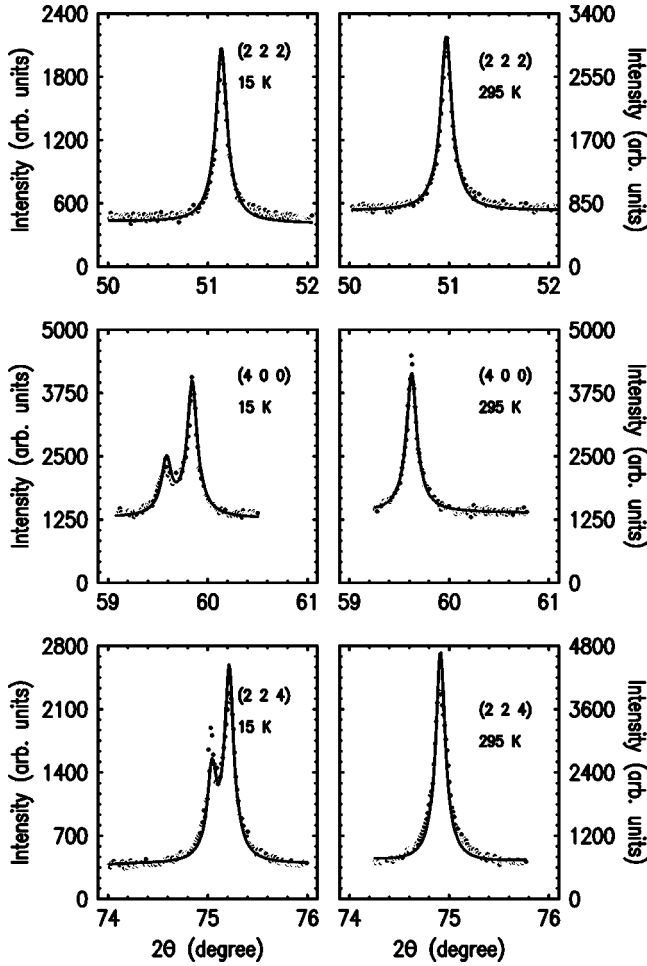


FIG. 4. Parts of the diffraction patterns measured with Synchrotron radiation on a powder sample obtained by grinding a part of crystal A for composition $\text{Ba}_{0.68}\text{K}_{0.32}\text{BiO}_3$. The solid lines correspond to fits of the data with the Rietveld technique in space group $I4/mcm$. The notations of the reflections correspond to the undistorted cubic perovskite.

The data were fitted with the Rietveld technique, and satisfactory description is obtained in space group $I4/mcm$, whereas the fit within space group $Ibmm$ shows deficiencies and results into unrealistic orthorhombic splittings. In Fig. 4 some parts of the diffraction pattern are shown together with the Rietveld description in space group $I4/mcm$. The indices are given in cubic notation; the tetragonal lattice parameters are related to the cubic one by $c_t = 2a_c$ and $a_t = \sqrt{2}a_c$. The cubic $(222)_c$ reflection corresponds to $(404)_t$ in tetragonal notation and should not split in the tetragonal phase. Indeed this reflection remains unchanged when cooling from 295 to 15 K. In contrast, in an orthorhombic phase $(222)_c$ would split into $(404)_o$ and $(044)_o$. The cubic $(400)_c$ and $(224)_c$ reflections should split in the tetragonal phase into $(008)_t/(440)_t$ and $(408)_t/(624)_t$, respectively, as it is well described by the Rietveld fit (the description of the peak intensities is still suffering from single grain scattering effects). On the ground of these peak splittings we can exclude the orthorhombic space group.

A powder sample II, obtained from the opposite corner of crystal A yielded the same results. A sample cut from sample B revealed peak broadening upon cooling for the $(400)_c$ and

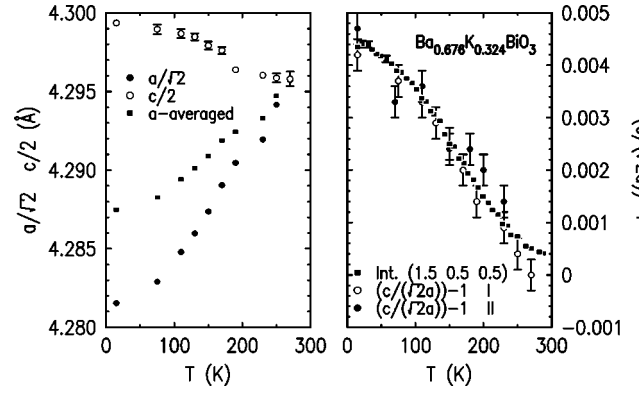


FIG. 5. Left part: temperature dependence of the lattice parameters determined by Synchrotron radiation on ground $\text{Ba}_{0.68}\text{K}_{0.32}\text{BiO}_3$. The tetragonal lattice parameters were rescaled to the undistorted cubic constant. Right part: temperature dependence of the tetragonal splitting defined as $c/\sqrt{2}a - 1$ (obtained on both samples) compared to the temperature dependence of the intensity of the $(1.5\ 0.5\ 0.5)$ -superstructure reflection intensity.

the $(224)_c$ cubic reflections whereas the $(222)_c$ reflection stayed unchanged. The reduced tetragonal splitting agrees with the smaller observed superstructure reflection intensity in this crystal, see Table I. The powder ground from a part of crystal D exhibited reflections widths too large for an analysis of these small splittings.

The transition from $Pm\bar{3}m$ to $I4/mcm$ is characterized by the condensation of a zone-boundary phonon mode, since it leads to a doubling of the translation cell. The corresponding phonon mode in the cubic phase is the triply degenerate rotation mode at the R point,^{5,14} associated with a three component order parameter. The condensation may lead to transitions into space groups $I4/mcm$, $Ibmm$, or $R\bar{3}c$ depending on the components of the order parameter which become nonzero.²⁶ In order to analyze the behavior of spontaneous strains one has to add coupling terms to the Landau-free energy.¹⁹ In the case of a zone boundary mode, any term linear in the order parameter is not invariant under the symmetry of the high temperature phase; therefore, the lowest allowed coupling is a term linear in the strain and quadratic in the order parameter ϵQ^2 . In addition one has to add the elastic energy caused by the strain given by the square of the strain times the corresponding elastic constant $C\epsilon^2$. The condition that the system has to be stress free $\partial F/\partial \epsilon = \partial/\partial \epsilon (a\epsilon Q^2 + C\epsilon^2) = 0$, leads to the proportionality between strain and the square of the order parameter

$$\epsilon \propto Q^2, \quad (4)$$

which may be easily verified by the superstructure reflection intensity, which is also proportional to the square of the order parameter. In Fig. 5 we show the temperature dependence of the tetragonal lattice parameters, which demonstrate the shrinking of the a, b plane due to the rotation of the octahedra around the c axis. In the right part of the figure the tetragonal strain is compared to the intensity of the superstructure reflection intensity, which confirms perfectly the expected relation (4). In the case of the orthorhombic phase one would expect a similar relation for the different ortho-

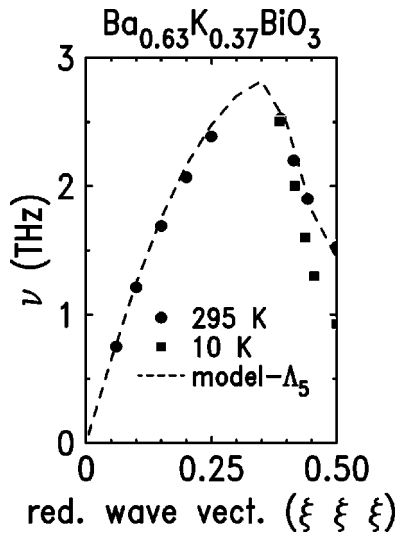


FIG. 6. Dispersion of the lowest (acoustic) Λ_5 branch in $\text{Ba}_{0.63}\text{K}_{0.37}\text{BiO}_3$, at the zone-boundary $R=(0.5\ 0.5\ 0.5)$ this branch ends in the triply degenerate rotation mode. The dashed line indicates the frequencies calculated with a shell model (Ref. 27).

rhombic strains, which was not found for samples at the border of the *Ibmm* phase in Ref. 8.

Summarizing the structural studies, one may conclude that there is a tetragonal phase between the *Ibmm* and the cubic phase, the latter should be restricted to much higher K content. In particular superconducting samples are still distorted at low temperatures. This distortion has certainly escaped detection in the previous powder diffraction experiments due to the low superstructure intensity combined with the small strains and/or a restriction to short range length scales. It appears tempting to identify the superconducting phase with the tetragonal space group, like it is proposed for BPBO.¹⁵ This resembles the interpretation of Pei *et al.*⁸ except that there is still a distortion (but different). The difference between nonsuperconducting and even nonmetallic BKBO and the superconducting samples would then be triggered by a different tilt scheme and, hence, resemble the suppression of superconductivity in the LTT phase of some cuprates.¹⁶ However, this idea needs certainly more detailed analysis. For instance there is significant spread in the literature on the K extension of the superconducting region in polycrystalline samples.^{28,29,1,7} Furthermore, there might be some difference in the *Ibmm*/*I4/mcm* phase boundary for powders and single crystals since this is a first order transition. Unfortunately, our attempts to grow single crystals in the *Ibmm* phase were not successful up to now.

Dynamics of the phase transition. Figure 6 shows the dispersion of the lowest (acoustic) Λ_5 branch measured on crystal D at 295 and at 10 K on the triple axis spectrometer 2 T. The branch ends at the *R* point (0.5 0.5 0.5) in the rotational mode, and it exhibits significant softening when approaching this mode. At both temperatures the dispersion shows the signature of a close structural instability. Furthermore, the dispersion can be well reproduced by the lattice dynamical model obtained by fitting the whole set of dispersion curves determined on the same crystal.^{14,27}

In Fig. 7 we show the temperature dependency of the frequency and that of the line-width of the rotation mode.

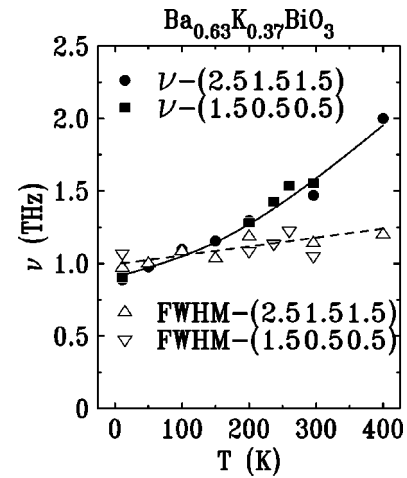


FIG. 7. Temperature dependence of the frequency and the width of the rotation mode at $R=(0.5\ 0.5\ 0.5)$ in $\text{Ba}_{0.63}\text{K}_{0.37}\text{BiO}_3$. The data were measured by constant Q scans on the thermal triple axis spectrometer 2T at two different Q values.

Surprisingly there is no indication of the structural transition occurring near ~ 220 K. In addition the mode remains strongly broadened (about four times the experimental resolution) in the entire temperature range. For a usual transition one would expect a frequency-softening of the mode upon cooling towards T_s and a splitting below T_s with one mode staying at low frequencies associated with the non-condensed components of the order parameter. This behavior is observed in SrTiO_3 .¹⁹ We think that the missing of a signature of the phase transition in the phonon modes in BKBO is another consequence of the huge structural disorder due to Ba-K mixing. Phonons are determined by the local structure on a time scale larger than their reciprocal frequency. Therefore, the pronounced critical quasielastic scattering has a similar influence on the phonon mode as the long range distortion below T_s . The character of the transition in these compounds has strong order-disorder character.

Simulation of the structural disorder by harmonic lattice dynamics. In a perfect crystal the atomic mean square displacements arise only from the thermal excitation of the phonon modes. Assuming harmonic lattice dynamics, which in the rather hard BKBO compounds is reasonably justified below room temperature, one may calculate the phonon contribution by a lattice dynamical model. Due to the determination of the entire phonon dispersion¹⁴ a reliable model for the lattice dynamics has been developed using the ionic charges, the shell charges and coupling to the cores, and the interaction potentials between the ions. Each phonon mode contributes to a mean square displacement along a defined direction of a certain ion, if the ion is displaced along this direction in the vibration, i.e., if the corresponding polarization vector component is nonzero. The integration of the polarization patterns of all branches weighted with the thermal occupation number over the Brillouin zone gives then the entire phononic contribution to the thermal parameter.

In Fig. 8 we compare the parameters as observed in the three four-circle experiments to these harmonic calculations (solid lines). The general tendency of the parameters is reflected in the calculated values, but there is a significant enhancement of the experimental mean square displacements

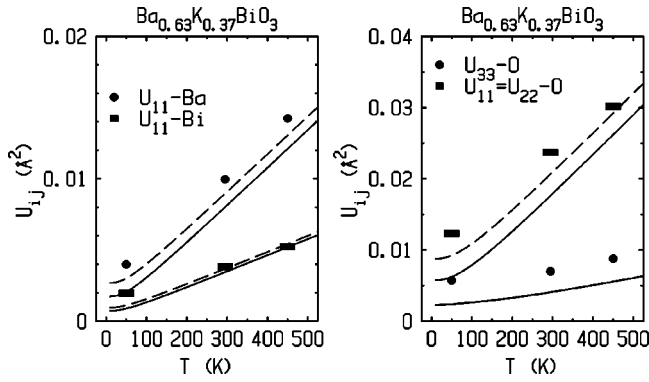


FIG. 8. Atomic displacement parameters for $\text{Ba}_{0.63}\text{K}_{0.37}\text{BiO}_3$ as a function of temperature. The symbols designate the values determined by elastic neutron diffraction; the solid lines indicate the contribution of phonons calculated in a harmonic lattice dynamical model and the dashed lines designate the phonon contribution added by the temperature independent square displacements induced by the Ba-K disorder. The disorder contribution was determined by relaxation of the local interactions in the harmonic model.

indicating additional disorder. For example, in the case of the HTCS cuprates^{30,31} much better agreement has been found in spite of a more complicated structure. The discrepancy most likely arises from the disorder induced by the Ba-K mixing, and is most pronounced for U_{11} of the oxygen, which is the parameter related to the octahedron rotation.

Using the harmonic model we have simulated the influence of the Ba-K mixing. For that purpose we have introduced distinct potentials for the Ba-O and the K-O interactions and distinct charges. Then large ($8 \times 8 \times 8$) supercells have been constructed with an arbitrarily fixed occupation of the A site by Ba and K ions. These cells contain 512 unit cells and 2560 sites. Corresponding to the K content of $x = 0.4$, 307 Ba atoms and 205 K atoms are distributed randomly to the A sites. The variation of the interatomic potentials results in nonzero forces on the ions, when these are fixed to values of the perovskite structure. We then allow the ions to relax these forces by positional displacements, whose squares were averaged over the supercell. After ten iterations the average force was reduced to about 0.005 eV/\AA corresponding to an average accuracy in the position of about 0.0005 \AA . The relaxation process was done exclusively in direct r space which does not provide an essential problem for $\text{Ba}_{0.6}\text{K}_{0.4}\text{BiO}_3$ due to the strong screening of the Coulomb potentials. Nevertheless, interactions up to 20 \AA had to be taken into account. In general, screening was accounted for by a Lindhard-type function (with a Fermi vector of $k_f = 0.45 \text{ \AA}^{-1}$ and a screening vector of $k_s = 0.49 \text{ \AA}^{-1}$) which is given in reciprocal space. The calculation uses the assumption that the ratio of the effective ionic charges corresponds to that of the nominal valences, in this case $Z(\text{Ba})/Z(\text{K}) = 2$. For identical ionic radii also the prefactors of the Born-Mayer potentials must have the same ratio within the framework of transferable potentials.

By performing this procedure for a large number of arbitrarily chosen supercells and by averaging the results, one may suppress the peculiarities of a certain configuration and gets the mean square displacements induced by the disorder in the interaction. We obtain for Ba/K $\Delta U = 0.00095 \text{ \AA}^2$ for Bi $\Delta U = 0.00023 \text{ \AA}^2$ and for O $\Delta U_{11} = 0.00301 \text{ \AA}^2$ per-

pendicular and $\Delta U_{33} = 0.00003 \text{ \AA}^2$ parallel to the Bi-O bond. The addition of these values to the temperature dependent phononic contribution describes the observed parameters reasonably well. In particular it may account for a large part of the enhancement of $U_{11}(\text{O})$, the thermal parameter related to the octahedron rotation. Most of the thermal parameters can hence be explained by the harmonic lattice dynamics and the Ba-K mixing. That the $U_{11}(\text{O})$ value is still larger than the calculation is certainly due to the anharmonic potentials related to the tilt, which are completely neglected in our model.

The influence of the Ba-K mixing $\text{Ba}_{0.63}\text{K}_{0.37}\text{BiO}_3$ can be estimated by comparing the static averaged oxygen displacement in the distorted phase 0.14 \AA , to the disorder induced root mean square displacement of 0.08 \AA as determined by the difference between phononic and measured mean square displacement. The disorder induced local variation of the rotation is comparable to its mean value. Therefore, it is not astonishing that the critical character of the phase transition is that anomalous. The fluctuations appear to be strongly pinned by the local disorder. Local disorder has also been conjectured from EXAFS studies.¹¹

The only thermal parameter whose enhancement may not be explained at all within this model is the oxygen value parallel to the bond. This enhancement might arise from damped or quasistatic breathing-type fluctuations and is reflected in anomalies in the phonon dispersion. The Bi-O-bond stretching vibrations, which are associated with the different types of breathing instability are found to be strongly renormalized in the metallic phase indicating a particularly strong electron phonon coupling⁵ in agreement with band structure calculations.³⁵

IV. CONCLUSION

The combination of neutron and synchrotron diffraction studies on BKBO clearly indicates that there still is a structural distortion in superconducting samples arising from an octahedron rotation. The local disorder induced by the mixing of Ba and K atoms on the same site essentially modifies the character of this *a priori* displacive phase transition. The transition is smeared and the expected phonon softening does not occur. The symmetry of the distorted phase is tetragonal, space group $I4/mcm$, adding an additional structure between the known orthorhombic and undistorted cubic phases. The structural distortion in this tetragonal space group represents the natural consequence of a rotational instability with the sequence $Pm\bar{3}m-I4/mcm-Ibmm$, since the direct transition $Pm\bar{3}m-Ibmm$ is not allowed by Landau-theory to be continuous.²⁶ The phase diagram of BKBO, therefore, resembles that of BPBO even more than previously thought and one might argue that just the change of the tilt direction triggers the different physical properties, i.e., metallic in $I4/mcm$ and nonmetallic in $Ibmm$. There have been serious efforts to study the metal insulator transition by optical methods^{32,12,13,33,34} and by EXAFS.¹⁰ These results indicate that the transition is associated with the disappearance of a short range breathing distortion which appears to be stabilized in the orthorhombic structure,^{7,8} i.e., by the tilt around an axis parallel to an octahedron edge. A connection between the tilt and the breathing instability was also conjectured

from band structure calculations³⁵ which concluded that the tilt is favorable for a breathing distortion. It appears highly desirable to study single crystalline samples close to the metal insulator transition by neutron scattering, however, these samples appear to be extremely difficult to prepare. But even in the superconducting samples studied here we find an enhanced value for the θ thermal parameter parallel to the Bi-O bond which indicates some persisting breathing distortion.

The dependence of electronic properties on the tilt scheme

suggests an analogy with nonsuperconducting cuprates, where charge order of the stripe-type has been observed,^{16,36} since in this case it is argued that the particular tilt scheme stabilizes the charge order related to a one-dimensional breathing distortion.

ACKNOWLEDGMENTS

We are grateful to W. Schmidbauer for providing us a crystal of good superconducting properties.

- ¹R.J. Cava, B. Batlogg, J.J. Krajewski, R. Farrow, L.W. Rupp, Jr., A.E. White, K. Short, W.F. Peck, and T. Kometani, *Nature* (London) **332**, 814 (1988).
- ²L.F. Mattheiss, E.M. Gyorgy, and D.W. Johnson, Jr., *Phys. Rev. B* **37**, 3745 (1988).
- ³D.G. Hinks, D.R. Richards, B. Dabrowski, D.T. Marx, and A.W. Mitchell, *Nature* (London) **335**, 419 (1988).
- ⁴C.-K. Loong, P. Vashishta, R.K. Kalia, M.H. Degani, D.L. Price, J.D. Jorgensen, D.G. Hinks, B. Dabrowski, A.W. Mitchell, D.R. Richards, and Y. Zheng, *Phys. Rev. Lett.* **62**, 2628 (1989); C.-K. Loong, P. Vashishta, R.K. Kalia, Wei Jin, M.H. Degani, D.G. Hinks, D.L. Price, J.D. Jorgensen, B. Dabrowski, A.W. Mitchell, D.R. Richards, and Y. Zheng, *Phys. Rev. B* **45**, 8052 (1992).
- ⁵M. Braden, W. Reichardt, A.S. Ivanov, and A.Yu. Rumiantsev, *Europhys. Lett.* **34**, 531 (1996).
- ⁶B. Battlog, R.J. Cava, L.W. Rupp, Jr., A.M. Musjce, J.J. Krajewski, J.P. Remeika, W.F. Peck, A.S. Cooper, and G.P. Espinosa, *Phys. Rev. Lett.* **61**, 1670 (1988).
- ⁷D.G. Hinks, B. Dabrowski, J.D. Jorgensen, A.W. Mitchell, D.R. Richards, Shiyou Pei, and Donglu Shi, *Nature* (London) **333**, 836 (1988).
- ⁸Shiyou Pei, J.D. Joergensen, B. Dabrowski, D.G. Hinks, D.R. Richards, A.W. Mitchell, J.M. Newsam, S.K. Sinha, D. Vaknin, and A.J. Jacobson, *Phys. Rev. B* **41**, 4126 (1990).
- ⁹D.E. Cox and A.W. Sleight, *Solid State Commun.* **19**, 969 (1976); E. Jurczek and T.M. Rice, *Europhys. Lett.* **1**, 225 (1986).
- ¹⁰S. Salem-Sugui, E.E. Alp, S.M. Mini, M. Ramanathan, J.C. Campuzano, G. Jennings, M. Faiz, S. Pei, B. Dabrowski, Y. Zheng, D.R. Richards, and D.G. Hinks, *Phys. Rev. B* **43**, 5511 (1991).
- ¹¹Y. Yacoby, S.M. Heald, and E.A. Stern, *Solid State Commun.* **101**, 801 (1997).
- ¹²K.F. McCarty, H.B. Radousky, D.G. Hinks, Y. Zheng, A.W. Mitchell, T.J. Folkerts, and R.N. Shelton, *Phys. Rev. B* **40**, 2662 (1989).
- ¹³S. Tajima, M. Yoshida, N. Koshizuka, H. Sato, and S. Uchida, *Phys. Rev. B* **46**, 1232 (1992).
- ¹⁴M. Braden, W. Reichardt, W. Schmidbauer, A.S. Ivanov, and A.Yu Rumiantsev, *J. Supercond.* **8**, 595 (1995).
- ¹⁵D.T. Marx, P.G. Radaelli, J.D. Jorgensen, R.L. Hitterman, D.G. Hinks, Shiyou Pei, and B. Dabrowski, *Phys. Rev. B* **46**, 1144 (1992).
- ¹⁶J.D. Axe, A.H. Moudden, D. Hohlwein, D.E. Cox, K.M. Mohanty, A.R. Moodenbaugh, and Youwen Xu, *Phys. Rev. Lett.* **62**, 2751 (1989); M.K. Crawford, R.L. Harlow, E.M. McCarron, W.E. Farneth, J.D. Axe, H. Chou, and Q. Huang, *Phys. Rev. B* **44**, 7749 (1991); B. Büchner, M. Cramm, M. Braden, W. Braunschweig, O. Hoffels, W. Schnelle, R. Müller, A. Freimuth, W. Schlabit, G. Heger, D.I. Khomskii, and D. Wohlleben, *Europhys. Lett.* **21**, 953 (1993).
- ¹⁷S.N. Barilo, V.I. Gatakskaya, S.V. Shiryayev, A.S. Shestac, L.A. Kurochkin, T.V. Smirnova, V.T. Koyava, N.S. Orlova, and A.V. Pushkarev, *Physica C* **254**, 181 (1995).
- ¹⁸W. Schmidbauer, A.J.S. Chowdhury, F. Wondre, B.M. Wanklyn, and J.W. Hoody, *Physica C* **235**, 759 (1994).
- ¹⁹A.D. Bruce and R.A. Cowley, *Structural Phase Transitions* (Taylor and Francis, London, 1981).
- ²⁰R.D. Shannon, *Acta Crystallogr., Sect. A: Cryst. Phys., Diffraction, Theor. Gen. Crystallogr.* **32**, 751 (1976).
- ²¹W. Kleemann, *Int. J. Mod. Phys. B* **7**, 2469 (1993).
- ²²U.H. Zucker, E. Perrenthaler, W.F. Kuhs, R. Bachmann, and H. Schulz, *Appl. Crystallogr.* **16**, 358 (1983).
- ²³The twinning in the 50 K data results in a correlation in the oxygen occupations preventing a reliable determination.
- ²⁴M. Braden, G. Heger, P. Schweiss, Z. Fisk, K. Gamayunov, I. Tanaka, and H. Kojima, *Physica C* **191**, 455 (1992).
- ²⁵G.H. Kwei, J.A. Goldstone, A.C. Lawson, J.D. Thompson, and A. Williams, *Phys. Rev. B* **39**, 7378 (1989).
- ²⁶H.T. Stokes and D.M. Hatch, *Isotropy Subgroups of the 230 Crystallographic Space Groups* (World Scientific, Singapore, 1988).
- ²⁷W. Reichardt and M. Braden (unpublished).
- ²⁸Y. Idemoto, Y. Iwata, and K. Fueki, *Physica C* **222**, 257 (1994).
- ²⁹W.D. Mosley, J.W. Dykes, P. Klavins, R.N. Shelton, P.A. Sterne, and R.H. Howell, *Phys. Rev. B* **48**, 611 (1993).
- ³⁰M. Braden, P. Schweiss, G. Heger, W. Reichardt, Z. Fisk, K. Gamayunov, I. Tanaka, and H. Kojima, *Physica C* **223**, 396 (1994).
- ³¹P. Schweiss, W. Reichardt, M. Braden, G. Collin, G. Heger, H. Claus, and A. Erb, *Phys. Rev. B* **49**, 1387 (1994).
- ³²S.H. Blanton, R.T. Collins, K.H. Kelleher, L.D. Rotter, Z. Schlesinger, D.G. Hinks, and Y. Zheng, *Phys. Rev. B* **47**, 996 (1993).
- ³³M.A. Karlow, S.L. Cooper, A.L. Kotz, M.V. Klein, P.D. Han, and D.A. Payne, *Phys. Rev. B* **48**, 6499 (1993).
- ³⁴A.V. Puchkov, T. Timusk, W.D. Mosley, and R.N. Shelton, *Phys. Rev. B* **50**, 4144 (1994).
- ³⁵A.I. Liechtenstein, I.I. Mazin, C.O. Rodriguez, O. Jepsen, O.K. Andersen, and M. Methfessel, *Phys. Rev. B* **44**, 5388 (1988); K. Kunc, R. Zheyner, A.I. Liechtenstein, M. Methfessel, and O.K. Andersen, *Solid State Commun.* **80**, 325 (1991).
- ³⁶J.M. Tranquada, B.J. Sternlieb, J.D. Axe, Y. Nakamura, and S. Uchida, *Nature* (London) **375**, 561 (1995).